nature geoscience

LETTERS

PUBLISHED ONLINE: 20 APRIL 2014 | DOI: 10.1038/NGEO2141

Mega-heatwave temperatures due to combined soil desiccation and atmospheric heat accumulation

Diego G. Miralles[1,2]*, Adriaan J. Teuling[3], Chiel C. van Heerwaarden[4] and Jordi Vilà-Guerau de Arellano[5]

The recent European mega-heatwaves of 2003 and 2010 broke temperature records across Europe[1–5]. Although events of this magnitude were unprecedented from a historical perspective, they are expected to become common by the end of the century[6,7]. However, our understanding of extreme heatwave events is limited and their representation in climate models remains imperfect[8]. Here we investigate the physical processes underlying recent mega-heatwaves using satellite and balloon measurements of land and atmospheric conditions from the summers of 2003 in France and 2010 in Russia, in combination with a soil–water–atmosphere model. We find that, in both events, persistent atmospheric pressure patterns induced land–atmosphere feedbacks that led to extreme temperatures. During daytime, heat was supplied by large-scale horizontal advection, warming of an increasingly desiccated land surface and enhanced entrainment of warm air into the atmospheric boundary layer. Overnight, the heat generated during the day was preserved in an anomalous kilometres-deep atmospheric layer located several hundred metres above the surface, available to re-enter the atmospheric boundary layer during the next diurnal cycle. This resulted in a progressive accumulation of heat over several days, which enhanced soil desiccation and led to further escalation in air temperatures. Our findings suggest that the extreme temperatures in mega-heatwaves can be explained by the combined multi-day memory of the land surface and the atmospheric boundary layer.

During the first days of August 2003, Europe experienced a devastating heatwave that brought on unparalleled consequences in terms of crop loss, wild fires, air pollution, transport disruptions and water scarcity. Estimates referred to a death toll of tens of thousands and an approximate US$10 billion economic loss[5,9]. Although the 2003 event was unprecedented at the time[5,7], a more prolonged and widespread heatwave struck Russia and Eastern Europe in 2010 (refs 1,3). To improve our predictability of these climate extremes, recent scientific efforts have concentrated on investigating their triggers and drivers[10–12]. The presence of high-pressure areas is a requirement for their occurrence[13]—both the 2003 and 2010 mega-heatwaves were associated with atmospheric blocking patterns, reduced cloudiness and advection of warm air[1,5,9]. Under these persistent synoptic conditions, the depletion of soil moisture and subsequent reduction in evaporative cooling may further amplify air temperatures[10,11]. This process is referred to as soil moisture–temperature feedback[10,12,14–16] and has been proposed as a key to the development of mega-heatwaves using indirect meteorological observations[10,12,17] and climate models[9,18]. Here, we combine multi-scale (surface and air) observations from both mega-heatwaves within a mechanistic framework to give new evidence of the land–atmospheric interactions and atmospheric boundary layer (ABL) dynamics that dominate these events.

Previous studies have pointed to the large variability in soil moisture in mid-latitude regions as a reason for their larger predisposition to experiencing mega-heatwaves[6,16]. Figure 1 offers a historical perspective (1980–2011) of the statistical coupling between soil moisture and summer air temperatures in Europe. The coupling diagnostic π (ref. 10) expresses the co-variability of the anomalies in afternoon air temperature (T') and the anomalies in the contribution of soil dryness to the surface sensible heat flux (e')—here π is derived using reanalysis[19] and satellite data[20] (Methods). The unprecedentedly high values of π during the summers of 2003 and 2010 indicate that when the extreme high temperatures occurred, soils were extraordinarily dry and yielding a large flux of sensible heat. The strength of this coupling is similar for the heatwaves of 2003 and 2010, suggesting an analogous role of soil moisture in the intensification of temperatures in both heatwaves. However, the coupling extended over a longer period and over a larger area in 2010, indicating a more persistent synoptic situation. In fact, a detailed insight reveals that blocking synoptic

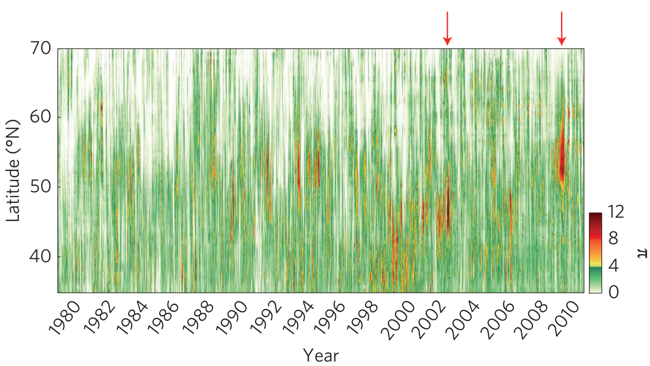

Figure 1 | Summer soil moisture–temperature coupling during 1980–2011 in Europe. Maximum value of the π daily coupling metric[10] per 0.25° latitude for the months from June to August. The 2003 and 2010 mega-heatwaves are indicated by red arrows.

[1]School of Geographical Sciences, University of Bristol, Bristol, BS8 1SS, United Kingdom, [2]Laboratory of Hydrology and Water Management, Ghent University, B-9000 Ghent, Belgium, [3]Hydrology and Quantitative Water Management Group, Wageningen University, 6709PA Wageningen, The Netherlands, [4]Max Planck Institute for Meteorology, 20146 Hamburg, Germany, [5]Meteorology and Air Quality Section, Wageningen University, 6709PA Wageningen, The Netherlands. *e-mail: diego.miralles@bristol.ac.uk

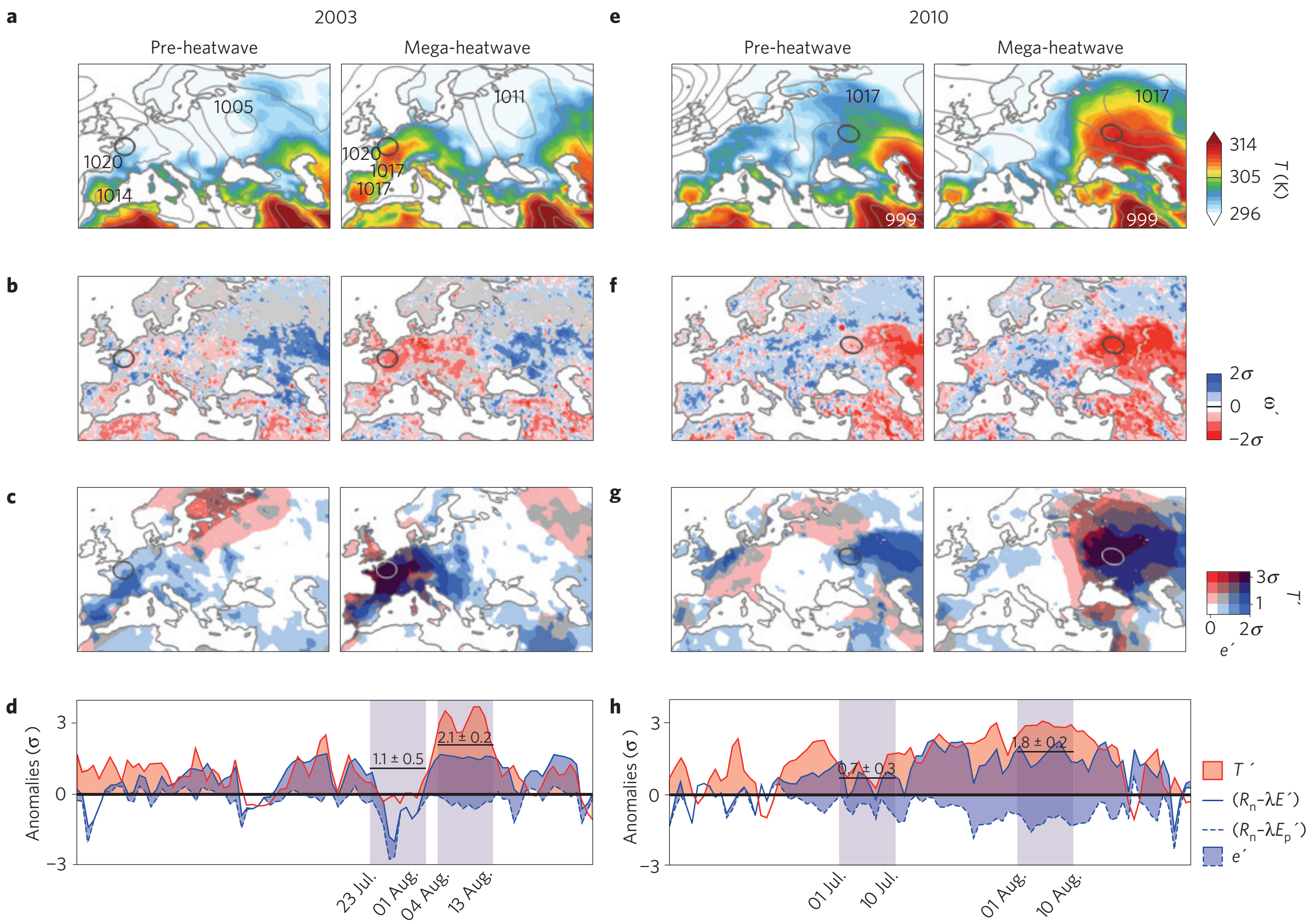

Figure 2 | Air temperature and soil moisture in Europe during recent mega-heatwave summers. a–d, Data for 10-day pre-heatwave (23 July–1 August) and mega-heatwave (4–13 August) periods in 2003: average afternoon near-surface air temperature[19] (T, K) and mean sea-level pressure[19] (hPa) (**a**); anomalies in surface soil moisture[30] (ω'), expressed in the number of standard deviations (σ) (**b**); co-variability of the T anomalies (T', σ) and the anomalies in the contribution of soil moisture deficit to the surface sensible heat flux[20] (e', σ) (**c**); and evolution of T' and e' for an area of 200 km radius around Trappes (marked in **a**–**c**) (**d**). R_n is surface net radiation, λE is latent heat flux and λE_p is latent heat flux based on potential evaporation. **e**–**h**, Same as **a**–**d** but for a 10-day pre-heatwave (1–10 July) and mega-heatwave (1–10 August) period in 2010; the focus region in **h** is the 200 km radius around Voronezh (marked in **e**–**g**). The horizontal black lines in **d** and **h** indicate the mean Bowen ratio $\pm 1\sigma$ for each 10-day period.

conditions were more dominant in 2010, allowing a continuous southerly advection of warm air (Fig. 2a,e). Conversely, in 2003 the wind direction and the strength of the convection was also affected by the formation of mesoscale thermal lows, low-pressure areas characteristic of very dry soils and intense ABL growth[21] (see Iberian Peninsula and southern France in Fig. 2a).

Despite these apparent differences, we also find ostensible similarities in the large-scale evolution of both mega-heatwaves. Maximum temperatures developed between high- and low-pressure systems, which allowed a combination of clear skies, low levels of subsidence and warm air advection. As a consequence of the high atmospheric demand for water, soil desiccation intensified (Fig. 2b,f), thus local land–atmospheric feedbacks progressively strengthened[16,18]. An analysis of the spatial distribution of the two separate components of the π coupling metric (that is, T' and e') shows that T' exceeded 3 standard deviations (σ) over extended regions during the peak of the events (Fig. 2c,g), with extreme statistical outliers of 5σ reached locally on certain days (in line with previous reports for the 2003 heatwave[7]). Interestingly, the regions where soil dryness had a strong effect on the surface energy balance (that is, high e')—already before the events (left panels in Fig. 2c,g)—recorded the highest absolute temperatures during the events (see right panels in Fig. 2a,e). To disentangle these land–atmospheric interactions and examine their impact in greater detail, hereafter we focus on two locations which have routine balloon-sounding stations and are representative of the broader areas affected by the events (Supplementary Figs 5 and 6): the cities of Trappes (30 km west of Paris) and Voronezh (500 km south of Moscow). During summer 2003, an area of 200 km radius around Trappes showed a coinciding peak in the daily dynamics of T' and e' (Fig. 2d)—the same occurred in Voronezh during 2010, but with a more prolonged and steady increase in both variables (Fig. 2h).

Night-time (00Z) sounding measurements of potential temperature (θ) and specific humidity (q) from Trappes (2003) and Voronezh (2010) also coincide in their patterns (Fig. 3a,b and Supplementary Fig. 4). The period before the heatwaves shows steady nocturnal lapse rates of $\sim$4 K km^{-1} (Fig. 3a). During the events, however, deep and warm nocturnal residual layers form, remaining decoupled from the surface by a strong ground thermal inversion (Fig. 3a). Such residual layers often occur over very dry soils[22] and can be further enhanced by mesoscale thermal lows[21]. They have the potential to intensify diurnal temperatures by storing heat from one day to the next: when the diurnal convection breaks the night ground inversion, the warm air from the residual layer is merged again into the diurnal ABL. The importance of these deep residual layers for the heat build-up during mega-heatwaves

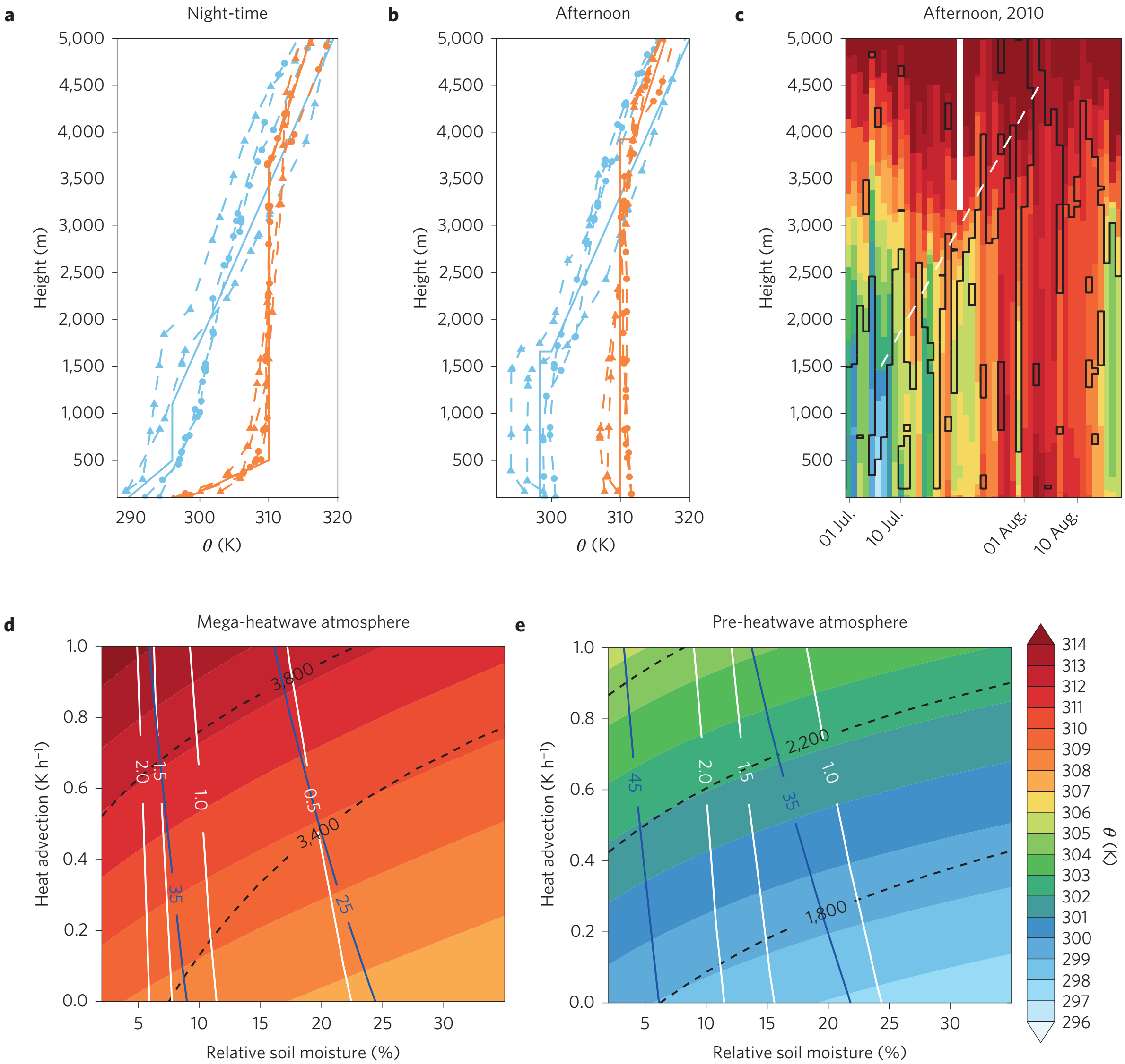

Figure 3 | ABL conditions during recent mega-heatwaves. a, Representative night-time (00Z) soundings of potential temperature (θ) from Trappes in 2003 (triangles) and Voronezh in 2010 (circles), during pre-heatwave (blue) and mega-heatwave (orange) periods. Solid lines indicate model initial conditions. **b**, Same but for the afternoon (12Z). **c**, Multi-day evolution of the afternoon θ profiles from Voronezh (2010). Black contours at 1.2 K km^{-1} indicate θ gradients; the white dashed line illustrates the multi-day increase in ABL height. **d–e**, Sensitivity of the ABL to soil moisture content and heat advection using the mega-heatwave (**d**) and pre-heatwave (**e**) initial conditions. Lines represent Bowen ratios (white), heat entrainment (blue, W m^{-2}) and ABL heights (black dashed, m); shading indicates afternoon ABL θ.

has not been investigated yet, although their presence was already noticed for the 2003 event[23]. The θ sounding profiles also reveal a strong diurnal ABL anomaly (Fig. 3b); although characteristic afternoon ABL heights at the latitudes of Trappes and Voronezh are below 2 km (as observed for the pre-heatwave periods), during the 2003 and 2010 events they reached almost 4 km—values more typical of (semi-)arid regions[22–24]. Based on the sounding measurements at Voronezh, Fig. 3c shows a monotonic multi-day increase in afternoon θ and ABL heights as the 2010 mega-heatwave strengthened.

Nonetheless, a purely observational analysis cannot reveal to what extent extreme mega-heatwave temperatures occur as a result of coinciding deficits in soil moisture and the multi-day storage of heat in the ABL. To enable a direct physical interpretation of our observations, and be able to track the response of the atmosphere (for example, air temperature changes) to any sort of perturbation in the heat budget (for example, soil drying), we complement the analysis with experiments using a mechanistic model of the soil water–atmosphere column[24–26]. The strong similarities found in the atmospheric soundings and land-surface observations from 2003 and 2010 allow us to conceptualize both events jointly in two experiments: one characteristic of a pre-heatwave period, one of a mega-heatwave period. Model experiments are initialized based on representative night-time balloon soundings of θ and q for pre-heatwave and mega-heatwave conditions (as shown in Fig. 3a and Supplementary Fig. 4a), and modelled fluxes are constrained using our satellite-based estimates[20] of Bowen ratios (the ratio of sensible to latent heat flux)—note the near-doubling of the Bowen ratios found under mega-heatwave conditions (Fig. 2d,h), consistent with the values from eddy-covariance measurements for the 2003 heatwave[11]. Initialized by night-time soundings and constrained by satellite data, our model reproduces satisfactorily the diurnal evolution of the ABL both for pre-heatwave and mega-heatwave periods (Fig. 3b), yielding constant heat advection intensities of ~0.2 K h^{-1} that are consistent with the isobar charts in Fig. 2a,b (Methods). The good match between experiments

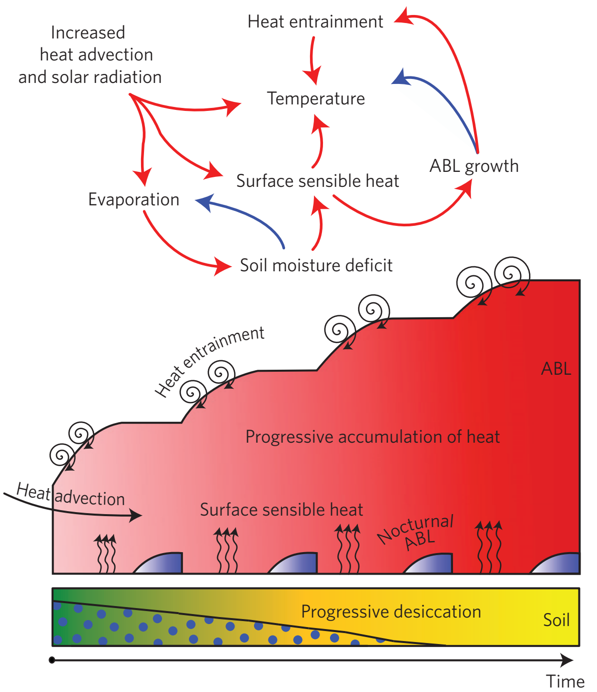

Figure 4 | Land–atmosphere interactions during mega-heatwaves revisited. Representation of the main soil moisture–air temperature interactions in the development of a mega-heatwave. Red and blue arrows represent positive and negative correlations, respectively.

and observations in Fig. 3b gives us confidence as to the model's ability to quantify the heat budget during mega-heatwaves (see also Supplementary Fig. 4b).

Next, we investigate the sensitivity of the model to changes in soil moisture and advection. First, by initializing the experiments using the mega-heatwave night-time conditions (orange line in Fig. 3a), we find that the observed afternoon temperatures exceeding 40 °C (313 K) at mid-latitudes can occur only under the cumulative effects of low soil moisture and high heat advection (Fig. 3d). Under these conditions, convection is intensified and the growth of the ABL is enhanced, leading to further entrainment of warm air from its top (which counteracts the increased dilution capacity of the ABL as it grows[24,27]). Second, by initializing our model using the pre-heatwave night-time sounding conditions (blue line in Fig. 3a), we find that afternoon temperatures are ~10 K lower (Fig. 3e). This shows that the storage of heat in the persistent nocturnal residual layer is key to explaining the escalation of temperatures during mega-heatwaves: without the multi-day accumulation of atmospheric heat, temperatures cannot escalate to reach the observed extremes. For the mega-heatwave experiment, we estimate a similar average diurnal contribution of heat into the ABL from surface sensible heat (~50%) and advection (~40%), and a lower contribution from entrainment (~10%), although these proportions vary greatly during the diurnal cycle.

Consequently, our results indicate that the record high temperatures of 2003 and 2010 occurred as a result of a combination of factors: the prevailing persistent synoptic patterns led to warm air advection and clear skies, the high atmospheric demand intensified soil desiccation (causing a strong surface sensible heat flux), the subsequent diurnal convection favoured the entrainment of warm air, and the formation of deep and warm nocturnal residual layers allowed the heat to re-enter the mixed layer in the following days. Soil moisture deficits have both direct and indirect effects in all these processes—effects that have not been scrutinized separately in previous model studies[9,18]. This suggests the need to revisit the traditional view of the soil moisture–temperature feedback during mega-heatwaves, in which only the direct impact of dry soils on the surface energy balance is explicitly considered[15,28].

Reinforced by our findings, a more complete conceptualization of the development of mega-heatwaves is provided in Fig. 4, with drying soils enhancing diurnal warm air entrainment and leading to the formation of persistent residual layers that favour the progressive build-up of atmospheric heat. This conceptualization provides a plausible answer as to why temperatures become increasingly higher as events evolve, and why they reach values that are so far outside the expected range of variability[1,7]. Our results do not suggest that a seasonal history of rainfall deficits is a necessary requirement (given the high atmospheric demand and fast soil dry-out in the early phases of the events), nor that soil desiccation plays an important role in the event duration, which seems ultimately determined by the synoptic conditions (see difference in length between the 2003 and 2010 events despite analogous land–atmospheric interactions). On the other hand, our results do indicate that the escalation of temperatures in mega-heatwaves can only be explained by considering the combined multi-day memory of land surface and ABL, and that improving the climate-model representation of land–atmosphere interactions is crucial to increasing our predictability of these events.

Methods

The π diagnostic of soil moisture–temperature coupling[10] (Fig. 1b) is the product of the anomalies in afternoon near-surface air temperature (T') and the anomalies in the effect of soil moisture deficits in the energy balance (e'). The latter is calculated as:

$$e' = (R_n - \lambda E)' - (R_n - \lambda E_p)' \tag{1}$$

where R_n refers to the surface net radiation, λE is latent heat flux and λE_p is the latent heat flux based on potential evaporation (E_p) instead of actual (E). Primes indicate the use of normalized anomalies expressed as the number of standard deviations relative to the multi-year (1980–2011) mean for each day of the year and a 31-day window moving average. Here, data of T and R_n come from ERA-Interim[19], while λE and λE_p come from GLEAM (refs 20,29) (all at 0.25° resolution). GLEAM is a satellite data-driven methodology based on a Priestley and Taylor formula to calculate E_p, which is then converted into E using a multiplicative evaporative stress factor derived from observations of vegetation water content, precipitation and surface soil moisture. Here, we use the GLEAM reference product with no data assimilation of soil moisture[29] to keep our coupling estimates independent of the surface soil moisture observations in Fig. 2b,f. For more details on GLEAM, and its forcing data and uncertainties, see Supplementary Information.

Our coupled model of the soil water–atmosphere column is a modelling system designed to study land–atmosphere interactions. It is based on a bulk representation of the conservation equations of momentum, heat and moisture in the atmosphere, and a force–restore model for soil heat and moisture[24–26]. The contributions of heat advection and soil moisture are treated as external forcing; here they are guided by the observed vertical profiles of θ and q, and by the Bowen ratios from GLEAM (Fig. 2d,h). Advection is assumed to occur only within the ABL and at constant rates during the day. The surface energy balance to calculate sensible, latent and ground heat fluxes uses net radiation as its input. This net radiation is the budget between: incoming shortwave (based on solar angle and transmissivity), outgoing shortwave (based on surface albedo), outgoing longwave (related to land surface temperature), and incoming longwave (based on atmospheric temperature). Both longwave components are solved using the Stefan–Boltzmann law. Initial and boundary conditions of our experiments are listed in Supplementary Tables 2 and 3.

Received 13 December 2013; accepted 14 March 2014; published online 20 April 2014

References

1. Barriopedro, D., Fischer, E. M., Luterbacher, J., Trigo, R. M. & García-Herrera, R. The hot summer of 2010: Redrawing the temperature record map of Europe. *Science* **332,** 220–224 (2011).
2. Dole, R. *et al.* Was there a basis for anticipating the 2010 Russian heat wave? *Geophys. Res. Lett.* **38,** L06702 (2011).
3. Coumou, D. & Rahmstorf, S. A decade of weather extremes. *Nature Clim. Change* **2,** 491–496 (2012).

4. Trenberth, K. E. & Fasullo, J. T. Climate extremes and climate change: The Russian heat wave and other climate extremes of 2010. *J. Geophys. Res.* **117,** D17103 (2012).
5. García-Herrera, R., Díaz, J., Trigo, R. M., Luterbacher, J. & Fischer, E. M. A review of the European summer heat wave of 2003. *Crit. Rev. Env. Sci. Tec.* **40,** 267–306 (2010).
6. Fischer, E. M. & Schär, C. Consistent geographical patterns of changes in high-impact European heatwaves. *Nature Geosci.* **3,** 398–403 (2010).
7. Schär, C. *et al.* The role of increasing temperature variability in European summer heatwaves. *Nature* **427,** 332–336 (2004).
8. Vautard, R. *et al.* The simulation of European heat waves from an ensemble of regional climate models within the EURO–CORDEX project. *Clim. Dynam.* **41,** 2555–2575 (2013).
9. Fischer, E. M., Seneviratne, S. I., Vidale, P. L., Lüthi, D. & Schär, C. Soil moisture–atmosphere interactions during the 2003 European summer heat wave. *J. Clim.* **20,** 5081–5099 (2007).
10. Miralles, D. G., van den Berg, M., Teuling, A. J. & De Jeu, R. A. M. Soil moisture–temperature coupling: A multiscale observational analysis. *Geophys. Res. Lett.* **39,** L21707 (2012).
11. Teuling, A. J. *et al.* Contrasting response of European forest and grassland energy exchange to heatwaves. *Nature Geosci.* **3,** 722–727 (2010).
12. Quesada, B., Vautard, R., Yiou, P., Hirschi, M. & Seneviratne, S. I. Asymmetric European summer heat predictability from wet and dry southern winters and springs. *Nature Clim. Change* **2,** 736–741 (2012).
13. Meehl, G. A. & Tebaldi, C. More intense, more frequent, and longer lasting heat waves in the 21st century. *Science* **305,** 994–997 (2004).
14. Mueller, B. & Seneviratne, S. I. Hot days induced by precipitation deficits at the global scale. *Proc. Natl Acad. Sci. USA* **109,** 12398–12403 (2012).
15. Seneviratne, S. I. *et al.* Investigating soil moisture–climate interactions in a changing climate: A review. *Earth Sci. Rev.* **99,** 125–161 (2010).
16. Seneviratne, S. I., Lüthi, D., Litschi, M. & Schär, C. Land–atmosphere coupling and climate change in Europe. *Nature* **443,** 205–209 (2006).
17. Hirschi, M. *et al.* Observational evidence for soil-moisture impact on hot extremes in southeastern Europe. *Nature Geosci.* **4,** 17–21 (2011).
18. Fischer, E. M., Seneviratne, S. I., Lüthi, D. & Schär, C. Contribution of land–atmosphere coupling to recent European summer heat waves. *Geophys. Res. Lett.* **34,** L06707 (2007).
19. Dee, D. P. *et al.* The ERA-Interim reanalysis: Configuration and performance of the data assimilation system. *Quart. J. R. Meteorol. Soc.* **137,** 553–597 (2011).
20. Miralles, D. G. *et al.* Global land-surface evaporation estimated from satellite-based observations. *Hydrol. Earth Syst. Sci.* **15,** 453–469 (2011).
21. Hoinka, K. P. & Castro, M. D. The Iberian Peninsula thermal low. *Quart J. R. Meteorol. Soc.* **129,** 1491–1511 (2006).
22. Santanello, J. A. Jr, Friedl, M. A. & Ek, M. B. Convective planetary boundary layer interactions with the land surface at diurnal time scales: Diagnostics and feedbacks. *J. Hydrometeorol.* **8,** 1082–1097 (2007).
23. Black, E., Blackburn, M., Harrison, G., Hoskins, B. & Methven, J. Factors contributing to the summer 2003 European heatwave. *Weather* **59,** 217–223 (2004).
24. Van Heerwaarden, C. C., de Arellano, J. V-G., Gounou, A., Guichard, F. & Couvreux, F. Understanding the daily cycle of evapotranspiration: A method to quantify the influence of forcings and feedbacks. *J. Hydrometeorol.* **11,** 1405–1422 (2010).
25. Tennekes, H. A Model for the dynamics of the inversion above a convective boundary layer. *J. Atmos. Sci.* **30,** 558–567 (1973).
26. De Arellano, J. V-G., van Heerwaarden, C. C. & Lelieveld, J. Modelled suppression of boundary-layer clouds by plants in a CO_2-rich atmosphere. *Nature Geosci.* **5,** 701–704 (2012).
27. Ouwersloot, H. G. & Vilà-Guerau de Arellano, J. Analytical solution for the convectively-mixed atmospheric boundary layer. *Bound.-Lay. Meteorol.* **148,** 557–583 (2013).
28. Alexander, L. Climate science: Extreme heat rooted in dry soils. *Nature Geosci.* **4,** 12–13 (2010).
29. Miralles, D. G. *et al.* El Niño–La Niña cycle and recent trends in continental evaporation. *Nature Clim. Change* **4,** 122–126 (2014).
30. Owe, M., de Jeu, R. & Holmes, T. Multisensor historical climatology of satellite-derived global land surface moisture. *J. Geophys. Res.* **113,** F01002 (2008).

Acknowledgements

This work is partly funded by the European Space Agency (ESA) WACMOS-ET project (contract no. 4000106711/12/I-NB). A.J.T. acknowledges support from The Netherlands Organization for Scientific Research (Veni grant 016.111.002). We thank R. d. Jeu for his feedback on the interpretation of soil moisture data, and W. v. d. Berg and J. Wisse for the interpretation of the synoptic situation. We acknowledge the University of Wyoming for making the balloon sounding data available at http://weather.uwyo.edu/upperair/sounding.html.

Author contributions

D.G.M., A.J.T. and J.V-G.d.A. jointly designed the study. D.G.M. led the large-scale analyses, A.J.T. the study of the sounding profiles, and J.V-G.d.A. the model experiments. C.C.v.H. contributed to the development of the atmospheric model. All co-authors contributed to the writing of the manuscript and the discussion and interpretation of results.

Additional information

Supplementary information is available in the online version of the paper. Reprints and permissions information is available online at www.nature.com/reprints. Correspondence and requests for materials should be addressed to D.G.M.

Competing financial interests

The authors declare no competing financial interests.